Intermediate Filaments in Small Configuration Spaces

Bernd Nöding and Sarah Köster*

Institute for X-Ray Physics and Courant Research Centre "Nano-Spectroscopy and X-Ray Imaging,"
Georg-August-Universität Göttingen, D-37077 Göttingen, Germany

Intermediate filaments play a key role in cell mechanics. Apart from their great importance from a biomedical point of view, they also act as a very suitable micrometer-sized model system for semiflexible polymers. We perform a statistical analysis of the thermal fluctuations of individual filaments confined in microchannels. The small channel width and the resulting deflections at the walls give rise to a reduction of the configuration space by about 2 orders of magnitude. This circumstance enables us to precisely measure the intrinsic persistence length of vimentin intermediate filaments and to show that they behave as ideal wormlike chains; we observe that small fluctuations in perpendicular planes decouple. Furthermore, the inclusion of results for confined actin filaments demonstrates that the Odijk confinement regime is valid over at least 1 order of magnitude in persistence length.

The cytoskeleton of eukaryotes includes three types of biopolymers: actin filaments, microtubules, and intermediate filaments (IFs). They have different mechanical properties and fulfill different functions in the cell. However, they all share the common trait of a large aspect ratio between length and diameter. Fibrous proteins govern virtually all cell mechanical aspects and are therefore of primary biomedical relevance. Importantly, they also provide a highly favored model system for studying polymer physics. The length of all three biopolymers lies in the range of many micrometers, and they can therefore conveniently be imaged by using state-of-the-art fluorescence microscopy. Whereas actin and tubulin are highly conserved, IF proteins share a common basic structure but occur in many different amino acid sequences, which are specific to different cell types. By this, IFs provide a "mechanical imprint" to cells, rendering them a particularly interesting candidate for cell mechanics research. The challenge arises to define general characteristics while still keeping the individual properties of each type of IF in focus. We choose to study vimentin IFs. Vimentin filaments are homopolymers and therefore have a simpler buildup than, e.g., keratin filaments. They are among the most abundant IFs in the human body. Moreover, vimentin is highly conserved in various species, implying an important physiological role [1,2]. However, we expect that the general results of this biopolymer study can be directly transferred to different types of IFs [3] or other semiflexible polymers.

In a biophysical context, actin filaments and vimentin IFs can be described as semiflexible polymers, since they have a persistence length L_P in the micron range. For actin filaments, a large number of studies have been carried out, and L_P has been determined to lie between 10 and 20 μm [4–7]. The mechanical properties of vimentin filaments have been studied on individual filaments by atomic force microscopy and electron microscopy and by bulk rheology methods. The authors find persistence lengths between 0.3 and 1 μm [8,9]. These investigations have tremendously furthered our understanding of the role IFs fulfill in the cell and of cell mechanics as a whole. However, the studies imply that individual filaments are either immobilized on a substrate to allow for atomic force microscopy or electron microscopy experiments or that they are studied in the context of a bulk sample. Therefore, direct interactions between the filament and the network or while the filament adsorbs on a surface have to be taken into account when interpreting the data, and deriving the isolated properties of the biopolymers becomes difficult. A direct measurement of freely fluctuating individual vimentin IFs addressing these issues is still largely missing.

Here we present a study on fluorescently labeled vimentin filaments [10] which are confined in narrow channels. We use the wormlike chain model including the confining channel geometry to describe the confined filaments [5,11]. The confining channels are included in the experiment for three main reasons. First, biopolymers in the cell are typically strongly confined by other cell components [12,13]; thus, the channels mimic this crowded environment. Second, from a polymer physics point of view, predictions for the behavior of semiflexible polymers in confinement have existed for many years, like the scaling law for wormlike chains introduced some 30 years ago by Odijk [14]. By comparing our data to actin data [5,11], we experimentally show that the relation is valid when each of the free parameters, persistence length and confinement strength, is varied. By additionally varying the height h of the microfluidic channels, we show that on the observed length scales the fluctuations in the focal plane and in the perpendicular plane decouple. Third, polymer studies rely strongly on statistically relevant amounts of data to obtain ensemble averages. By introducing the confining channels,

we initially reduce the configuration space of the polymer of length L from $\sim hL^2$ to $\sim hLd$. However, by taking into account de Gennes's idea to view the polymer as a chain of statistically independent "blobs" [15] which was applied to semiflexible chains by Odijk [14], the configuration space is reduced even more, by 2 orders of magnitude in total, to $\sim h\lambda d$. This is the case because the confined polymer chain can be viewed as a sequence of $N = L/\lambda$ "links" of deflection length λ. Therefore, by decreasing the configuration space, we introduce many repeat units and largely improve the statistics so that we are able to perform very precise measurements.

Human vimentin is recombinantly expressed in *E. coli* bacteria, purified from inclusion bodies [16] and labeled with AlexaFluor 488 C_5 maleimide (Invitrogen GmbH, Darmstadt, Germany). The labeling procedure is adapted from Ref. [10] with minor changes. For the filament assembly process, the protein concentration is adjusted to 0.4 mg/ml. The ratio for labeled to unlabeled protein is 3:1 to optimize both fluorescence intensity and assembly properties. The protein assembles in 2 mM phosphate buffer and 100 mM KCl at pH 7.5 and 37 °C for 18 hours in dialysis tubing, thus reducing the fluorescent background. Typical filament lengths vary between 5 and 40 μm, and for the analysis shown here we consider only filaments with a minimal length of 10 μm, most of them being longer than 15 μm. Comparison with unlabeled filaments [8] ensures that the mechanical properties of the filaments remain unaffected after labeling. Microfluidic channels with widths between 1.2 and 2.7 μm and heights of 0.45 or 1 μm are fabricated from polydimethylsiloxane by soft lithography methods [17,18] using SU-8 2000 negative photoresist. The microchannels are sealed with a glass cover slip and remain open on both ends [Fig. 1(a)]. Capillary forces are used to flush the channels first with 50 mg/ml bovine serum albumin solution preventing adsorption of vimentin to the channel walls and subsequently with vimentin filament solution at a protein concentration of 1–5 μg/ml. Fluorescently labeled filaments are imaged by using an Olympus CellR setup with a 60× oil immersion objective. 300–600 individual images per filament are recorded with an exposure time of 50 ms and a rate of 10 Hz, resulting in a total observation time of at least 30 s. These values ensure that the filament occupies a sufficient part of the configuration space in the channel. Figure 1(b) shows the influence of different degrees of confinement on individual filaments.

The raw microscopy images are processed to obtain smooth contours. From these contours, a tangent correlation function is calculated for every image series. The assembly process yields filaments of variable length [19]. However, our data (not shown) demonstrate that the results are independent of filament length. Therefore, the tangent correlation functions for filaments (20–70 individual filaments for each curve shown in Figs. 2 and 3 corresponding
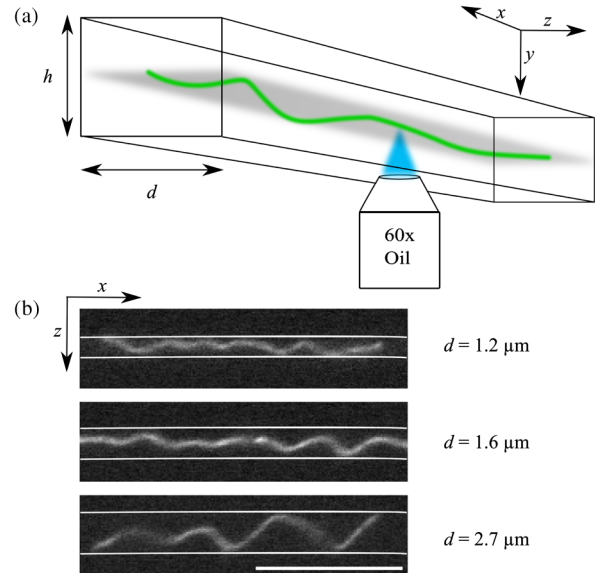

FIG. 1 (color online). (a) Sketch of the experimental situation. Fluorescently labeled filaments are confined in microchannels of varying widths d and heights h. (b) Fluorescence images of vimentin IFs confined in microchannels with different widths. Channel walls are indicated by white lines. The filaments' characteristic fluctuations change significantly with the width of the confining channel. (The scale bar indicates 10 μm.)

to more than 50 000 individual images) confined in channels of identical geometry (width and height) can be averaged by taking into account different statistical weights due to varying filament lengths. Results for three channel widths ($d = 1.2$ μm, $d = 1.6$ μm, and $d = 2.7$ μm) of uniform height ($h = 1$ μm) are plotted in Fig. 2 (open symbols). Overall, the correlation decreases with increasing channel width as can be predicted from Fig. 1(b). An analytical description yields

$$\langle\cos\theta(l)\rangle = 1 - \frac{\lambda}{2\sqrt{2}L_P}\left[\cos\left(\frac{\pi}{4}\right) - \cos\left(\frac{l}{\lambda} + \frac{\pi}{4}\right)\exp\left(\frac{-l}{\lambda}\right)\right]$$

(1)

for the tangent correlation function [5]. This function is obtained by assuming a parabolic potential of strength K for the channel walls. Two parameters, the persistence length L_P and the deflection length $\lambda = \sqrt{2}(\kappa/K)^{1/4}$ with the bending rigidity κ, are included. Values for both parameters are obtained through fitting of the data as shown in Fig. 2 (solid lines). The deflection length λ is dependent on the channel width, which is related to the potential strength K. However, L_P as a material property of vimentin filaments is constant; we obtain $L_{P(\text{conf})} = 2.1 \pm 0.1$ μm.

We compare this value to literature data for static measurements using electron microscopy and atomic force microscopy, $L_{P(\text{stat})} \approx 1$ μm [8]. The factor of 2 between $L_{P(\text{conf})}$ and $L_{P(\text{stat})}$ is likely to be due to the interaction of the filaments and the substrate and not to the labeling or to
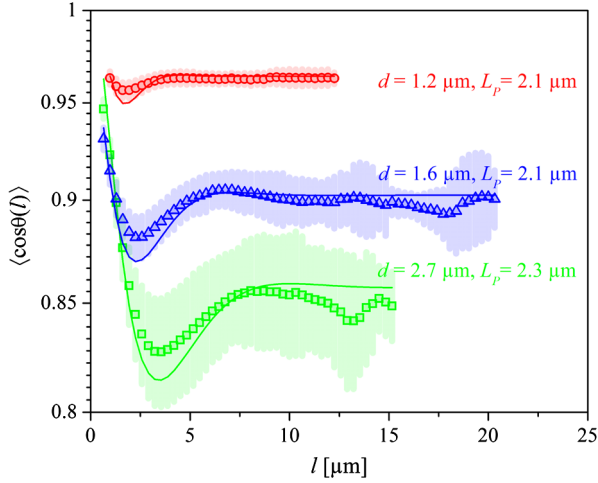
FIG. 2 (color online).   Tangent correlation functions for fila-ments in channels of different widths. Each curve shows data averaged from several measured filaments. The data are fitted with the analytical solution for a confined polymer in a parabolic potential. Error bars are indicated in a lighter color.
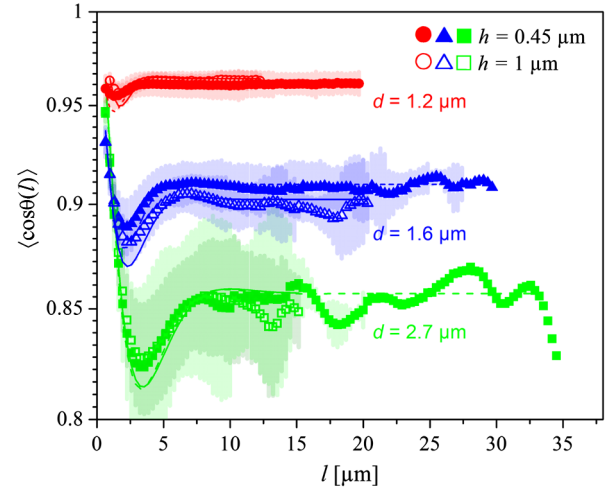

FIG. 3 (color online).   Pairs of tangent correlation functions of filaments confined in channels of two different heights but equal width show identical behavior. Error bars are indicated in a lighter color.

the confinement in the channels. This can be concluded from additional measurements on adherent fluorescent fil-aments on glass (data not shown) that by contrast to our nonadherent filaments have a smaller apparent $L_{P(\text{stat})} \approx$ 1 μm. Moreover, consistently with this argumentation we find that freely fluctuating, unconfined filaments restricted to the focal plane by two glass plates also yield a value of $L_{P(\text{unconf})} = 2.0 \pm 0.5$ μm. The comparably large error is a consequence of the fact that without channels the configu-ration space is considerably increased and a longer obser-vation time would be needed to guarantee equally accurate data. This circumstance, which argues strongly for de-creasing the configuration space, is also impressively illus-trated by the increased error range with increasing channel width; see Fig. 2.

The wormlike chain model used to derive Eq. (1) is valid in two dimensions. The reasoning behind this choice is that using fluorescence microscopy we observe the filaments in the focal plane and cannot image fluctuations in the per-pendicular direction. For small fluctuations only, as we ensure them by confining the filaments in narrow channels, Monge parametrization can be introduced, thereby project-ing the fluctuations in the y and z directions on the x axis. In this case, the y and the z components in the Hamiltonian describing the bending energy decouple, and consequently the projection of the 3D results to the 2D xz plane should be independent of the channel height.

It has been discussed to which extent confinement alters the *apparent* persistence length [20–22]. However, by ana-lyzing the (projected) data using the 2D wormlike chain model, we derive the intrinsic ("bulk") persistence length, which is a material property of the biopolymer. In our experiments, we compare two different channel heights, 0.45 and 1 μm, as shown in Fig. 3 (solid and open

symbols, respectively). The data curves agree very well. Importantly, if there were a coupling between the perpen-dicular directions of fluctuation, it should become apparent in differences between the data for different channel heights. However, this is not the case on the length scales accessible by our methods.

Apart from the persistence length L_P, confined biopol-ymers are described by the deflection length λ. A relation between both values and the channel width was introduced by Odijk through the scaling law [14]

$$\lambda = a d^{2/3} L_P^{1/3}. \qquad (2)$$

Here a is a geometry-dependent constant. We are now in the position to test this scaling law experimentally by varying both free parameters d and L_P. Since the latter is a material property, we include data of a second semi-flexible polymer, filamentous actin, which has been studied extensively in confinement in the past [5,11,13,23]. Vimentin IFs and actin filaments are ideal candidates for such a comparison, since their persistence lengths differ by about 1 order of magnitude. It has to be noted that the differences between both polymers lie not only in their mechanical properties but also in their molecular structure. Whereas the vimentin IF consists of rodlike subunits as-sembled in a hierarchical manner [24,25], the actin fila-ment consists of globular subunits that polymerize ATP-dependently [26]. Despite these striking differences, the geometry factor a remains constant for both biopolymers and for various values of d and h, as shown in Fig. 4. These results demonstrate the universal character of the scaling law and also prove that both actin filaments and vimentin IFs, despite their complex molecular architecture, can be described by the simple wormlike chain model.
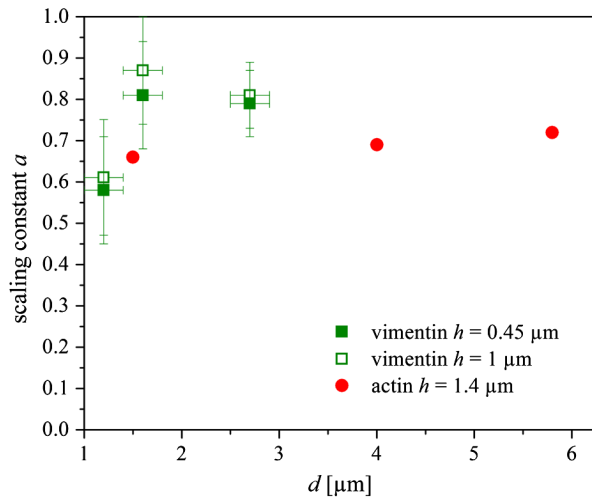
PHYSICAL REVIEW LETTERS

FIG. 4 (color online). Vimentin and actin filament properties are compared by using the scaling constant a from Odijk's scaling law. We find very similar values for the scaling constant for different confinement parameters and also for both vimentin and actin [5] filaments.

Vimentin filaments and other IFs are of great importance for biology and medicine due to their crucial role in the eukaryotic cell. From a more fundamental point of view, they are also an ideal model system to study the effect of confinement on (bio)polymers. Their persistence length is in the range of a few micrometers and short compared to their contour length (tens of micrometers) but still large enough so that fluctuations can be resolved by conventional fluorescence microscopy. Thereby, the usual assumption of "infinitely long" filaments in the wormlike chain model is much better realized than for, e.g., actin filaments on which most studies in the past have been carried out. We are able to show that on microscopic length scales the fluctuations in the focal plane and those in the perpendicular plane decouple; i.e., no influence of the channel height on the tangent correlation function can be observed. Therefore, the 2D wormlike chain model can be used to describe such microscopy data. Furthermore, by comparing two semiflexible biopolymers with persistence lengths of 15 and 2 μm, respectively, confined in the Odijk regime [27], the corresponding scaling law can be nicely confirmed. These conclusions are based on precise measurements which we are able to perform, since for confined semiflexible polymers the configuration space is considerably reduced as compared to freely fluctuating polymers.

*sarah.koester@phys.uni-goettingen.de

[1] H. Herrmann, B. Fouquet, and W. Franke, Development (Cambridge, U.K.) **105**, 279 (1989).
[2] M. Schaffeld, H. Herrmann, J. Schultress, and J. Markl, Eur. J. Cell Biol. **80**, 692 (2001).
[3] H. Bär, M. Schopferer, S. Sharma, B. Hochstein, N. Mücke, H. Herrmann, and N. Willenbacher, J. Mol. Biol. **397**, 1188 (2010).
[4] F. Gittes, B. Mickey, J. Nettleton, and J. Howard, J. Cell Biol. **120**, 923 (1993).
[5] S. Köster, D. Steinhauser, and T. Pfohl, J. Phys. Condens. Matter **17**, S4091 (2005).
[6] A. Ott, M. Magnasco, A. Simon, and A. Libchaber, Phys. Rev. E **48**, R1642 (1993).
[7] P. Venier, A. C. Maggs, M. F. Carlier, and D. Pantaloni, J. Biol. Chem. **269**, 13 353 (1994).
[8] N. Mücke, L. Kreplak, R. Kirmse, T. Wedig, H. Herrmann, U. Aebi, and J. Langowski, J. Mol. Biol. **335**, 1241 (2004).
[9] M. Schopferer, H. Bär, B. Hochstein, S. Sharma, N. Mücke, H. Herrmann, and N. Willenbacher, J. Mol. Biol. **388**, 133 (2009).
[10] S. Winheim, A. R. Hieb, M. Silbermann, E.-M. Surmann, T. Wedig, H. Herrmann, J. Langowski, and N. Mücke, PLoS ONE **6**, e19202 (2011).
[11] S. Köster, H. Stark, and T. Pfohl, Biophys. Rev. Lett. **2**, 155 (2007).
[12] D. C. Morse, Phys. Rev. E **63**, 031502 (2001).
[13] S. Köster and T. Pfohl, Cell Motil. Cytoskeleton **66**, 771 (2009).
[14] T. Odijk, Macromolecules **16**, 1340 (1983).
[15] P. G. de Gennes, *Scaling Concepts in Polymer Physics* (Cornell University, Ithaca, NY, 1979).
[16] H. Herrmann, L. Kreplak, and U. Aebi, Methods Cell Biol. **78**, 3 (2004).
[17] D. Duffy, J. McDonald, O. Schueller, and G. Whitesides, Anal. Chem. **70**, 4974 (1998).
[18] S. Quake and A. Scherer, Science **290**, 1536 (2000).
[19] S. Portet, N. Mücke, R. Kirmse, J. Langowski, M. Beil, and H. Herrmann, Langmuir **25**, 8817 (2009).
[20] J. Hendricks, T. Kawakatsu, K. Kawasaki, and W. Zimmermann, Phys. Rev. E **51**, 2658 (1995).
[21] P. Cifra, Z. Benková, and T. Bleha, J. Phys. Chem. **112**, 1367 (2008).
[22] P. Cifra, Z. Benková, and T. Bleha, Faraday Discuss. **139**, 377 (2008).
[23] S. Köster, J. Kierfeld, and T. Pfohl, Eur. Phys. J. E **25**, 439 (2008).
[24] S. Strelkov, H. Herrmann, and U. Aebi, BioEssays **25**, 243 (2003).
[25] H. Herrmann and U. Aebi, Curr. Opin. Struct. Biol. **8**, 177 (1998).
[26] K. C. Holmes, D. Popp, W. Gebhard, and W. Kabsch, Nature (London) **347**, 44 (1990).
[27] Y. Wang, D. Tree, and K. Dorfmann, Macromolecules **44**, 6594 (2011).